THEORETICAL STUDY OF POST EXIT BEHAVIOUR OF DROPLETS FROM A HIGH PRESSURE AGRO-FORESTRY SWIRL NOZZLE

A. Taiwo[1] and K. Oje[2]
[1]Department of Agricultural Engineering, Ladoke Akintola University of Technology, P.M.B. 4000, Ogbomoso, Oyo State, Nigeria. padetaiwo@yahoo.com
[2]Department of Agricultural and Biosystems Engineering, University of Ilorin, P.M.B. 1515, Ilorin, Kwara State, Nigeria. kayodeoje2@yahoo.com

ABSTRACT

A better understanding of the fundamental principles underlying the movement of droplets which escaped from the exit orifice of a high pressure agro-forestry swirl nozzle in still air was developed. Equations of dynamic systems of droplets distribution at high pressure were used in conjunction with particle dynamics equations to develop mathematical models of motion phenomenon of liquid droplets in still air. The models were implemented with algorithm coded in C++ language to investigate the effects of droplet diameter, nozzle supply pressure, and time variation on selected motion parameters of drag force, Reynolds number, final velocity and distance.

The simulation results established that while viscous forces are predominant on droplets whose diameters ranged between 100 and 200 microns when they move in still air, inertia forces are predominant on droplets whose diameters are larger. The drag force increased with increase in droplets diameters and nozzle supply pressure. For a 5 fold increase in droplet diameter under the same nozzle supply pressure, drag force increases by 20 times. The pattern of variation of final velocities of liquid droplets in terms of droplet diameter and nozzle supply pressure is similar to that of the distance traveled by the droplets. The practical implication of these results is that whenever it is necessary to produce droplets whose diameters fall within the range of 100 and 200 microns with an agro-forestry swirl nozzle, auxiliary air blast must be provided before they could hit the intended target(s).

KEYWORDS: Orifice, swirl nozzle, agro-forestry, droplets, knapsack sprayer, terminal velocity.

1. INTRODUCTION

Agro-forestry is a farming system that integrates crops and/or livestock with trees and shrubs. It creates a high quality matrix that increases the movement of animals from one protected area to another, thereby increasing the overall connectivity of natural habitats. It also reduces soil erosion and increases carbon sequestration, water uptake and storage. It provides economic benefits to farmers through the large diversity of crops produced (Rajankumar, 2007).

The major constraints to production in agro-forestry systems, among several others include: inadequate and unsatisfactory control of pests and diseases in tree crops, uncontrolled bush burning which kills non-target species which play a predatory role in the ecosystem under an Integrated Pest Management (IPM) system, and unsatisfactory regulation of moisture and control of temperature in livestock buildings and environments during the hot and dry seasons of the year (Adejumo, 2005; Kang, 1996).

Crop spraying, which is the application of certain organic and inorganic substances in solution form to combat insect pests and plants diseases of field and tree crops, remain the best option for controlling pests and pathogens in agro-forestry systems in Nigeria because of the annual recurrent problem of uncontrolled bush burning (Kang,1996; Shaip et. al, 1997). However, if adequate precautionary measures are not taken, up to 90% of the active ingredients sprayed for crop protection may never reach their intended targets due to drift (Bower et. al, 2001; Zhu et. al, 1994).

Presently in Nigeria, application of liquid chemical pesticide to tree crops and other components of agro-forestry system have been abandoned to the use of relatively ineffective and antiquated knapsack sprayers. This type of sprayer is seriously limited by the fact that it cannot get pesticide to targets located either on the canopies of tall tree crops or deep inside wide tree crowns. In addition, it has the built-in danger of depositing part of the pesticides (which are usually poisonous) on the surface of the operator's skin in the event of a leakage in its tank or reservoir. Even if there is no leakage in the tank, the liquid pesticide run-off from the recently-sprayed trees can easily be deposited on any part of the body of the applicator (Taiwo, 2009). This is completely unacceptable because most of such pesticides could be absorbed either directly or indirectly into the excretory and other organs of the applicator's body from where they can later travel down to more sensitive and vital organs to cause incalculable, and sometimes, irreparable damage if not outright death (UNCTAD, 2006; UNEP, 2008).

The best way to solve this problem is to develop a motorized high pressure agro-forestry sprayer which can be truck or tractor-mounted. Since the nozzle is the most critical component of any spraying apparatus, the starting point for the development of this type of sprayer is the development of the nozzle. The nozzle performs three major functions in the sprayer, namely: to regulate flow, atomize the mixture into droplets, and disperse the sprayer in a specific pattern (Osarenren and Ndukwe, 2002). Nozzles are of two basic types. According to Bernacki et al., (1972), the first type is a pressure nozzle, in which the liquid breaking process results from the conversion of its potential pressure energy into the potential energy of the surface tension of the droplets and, finally into their kinetic energy. The second type constitutes the hydro-pneumatic nozzles in which the liquid is broken into droplets as a result of the impact of a stream of air or some other gas against a thin layer of liquid delivered to the nozzle at a relatively low pressure.

Nozzles that produce flat sheets through the use of an elliptical orifice are referred to as fan, flat spray, or flat fan nozzles and those that produce flat sheets by a circular orifice adjacent to a deflector surface are referred to as flood, flooding or deflector nozzles (ASAE, 2002). Hollow cone-shaped liquid sheets are produced by imparting a swirling motion to the liquid as it exits the nozzle through the use of either a slotted swirl plate (or "element") in combination with a simple disc orifice or by a tangential liquid inlet into a swirl chamber and allowing the swirling liquid to exit through a circular orifice located at the end of the chamber. These nozzles are commonly referred to, respectively, as disc-core hollow cone nozzles and swirl or swirl chamber nozzles (ASAE, 2002).

Since a nozzle produces droplets with a wide range of sizes known as the droplet – size spectrum, this implies that in order to develop a nozzle, there is need to first of all study the behaviour of the various droplets sizes in still air, then study how the nozzle should perform to enable the droplets it discharge behave in a particular fashion, and finally study the geometrical configuration and material of the principal functional element of the nozzle required to enable the nozzle perform as it should. The objective of this research, therefore, was to study the theoretical behaviour of the droplets in still air after escaping from the exit orifice of a high pressure agro-forestry swirl nozzle. Specific objective was to study the effect of droplets diameter, nozzle supply pressure, and time variation on droplets' final velocity, distance, drag force, and Reynolds number.

2. MATERIALS AND METHODS

2.1 Theoretical Considerations

The movement of liquid droplet under the nozzle supply pressure (P_i) from the moment it breaks off from the discharging liquid stream as soon it flows out of the nozzle exit orifice have been exhaustively described by Awardy (1978); Lefebvre (1989); Goering et al. (1972); Koo and Kuhlman (1993); Bernacki et al. (1972). Following the studies above, the classical equation for drag (or air resistance) force on a droplet can be described as:

$$F_D = \frac{\pi}{8} C_d \rho_a V_0^2 D_p^2 \quad (1)$$

Where: F_D = Air Resistance or drag force (Newton); C_d = Dimensionless drag coefficient (-); ρ_a = Air density (kg/m^3); V_0 = Initial velocity of particle relative to the medium (air) (m/s); D_p = Diameter of Droplet (m); A_p = Projected area of the droplet perpendicular to the direction of flow (m^2).

Gravity and buoyancy forces were also easily accounted for in the cited works with the following equations:

$$W = g(\rho_l - \rho_a)\frac{\pi D_p^3}{6} \quad (2)$$

Where: W = Buoyancy and Gravity forces put together (Newton); ρ_l = Density of liquid in the droplet (kg/m^3); g = Acceleration due to gravity (m/s^2).

It was also established that the drag coefficient varied with Reynolds number depending on whether the flow was lamina, turbulent or transitional. In view of this it was proposed by Bernacki et al. (1972) that Reynolds number R_e could be calculated according to the following formula:

$$R_e = \frac{\rho_a V_0 D_p}{\eta_a} \quad (3)$$

Where: R_e = Reynolds Number; η_a = Dynamic viscosity of air.

Bernacki et al (1972); Lefebvre, (1989); Goering *et al* (1972) established the following criteria for Reynolds number and drag coefficient under the various flow types:

For flow in laminar or Stokes law region: $R_e \le 2$, $C_d = \frac{24}{R_e}$

For transitional or Allen flow region: $2 \le R_e \le 500$, $C_d = 0.4 + \frac{40}{R_e}$

For turbulent flow: $R_e > 500$, $C_d = 0.44$ (4)

It was also recognized that if the values of the criteria established in equation (4) were substituted into the formula for drag force or air resistance, the following relationships for air resistance (or drag force) will be obtained for each type of flow:

For Stokes law region: $F_D = 3\pi\eta_a V_0 D_p$

For Allen flow region: $F_D = \pi\left(0.05\rho_a V_0^2 D_p^2 + 5\eta_a V_o D_p\right)$

For turbulent low: $F_D = 0.055\pi\rho_a V_0^2 D_p^2$ (5)

The terminal or ultimate velocity, V_u of the moving droplet within the liquid stream occurs when the drag force becomes balanced by the gravitational forces. Bernacki et al. (1972); Lefebvre (1989) developed the equation for the ultimate velocity of the moving droplets with the liquid stream for Stokes law region, Allen flow region, and Turbulent flow regions as follows:

$$\left.\begin{aligned} &\text{For Stokes law region:} \quad V_u = \frac{gD_p^2(\rho_l - \rho_a)}{18\eta_a} \\ &\text{For Allen flow region:} \quad V_u = \sqrt{\frac{2500\eta_a^2}{\rho_a D_p^2} + \frac{gD_p(\rho_l - \rho_a)}{0.3\rho_a}} - \frac{50\eta_a}{\rho_a D_p} \\ &\text{For turbulent Flow:} \quad V_u = \sqrt{\frac{gD_p(\rho_l - \rho_a)}{0.33\rho_a}} \end{aligned}\right\} \quad (6)$$

From equation (6), it is possible to establish the limits of the lamina flow as well as the velocity of the falling droplets of different diameters. However, in the real world, there never comes a time when droplets generally come to a free fall because the velocities achieved in spraying are usually relatively high (Bode et al 1979), Bernacki et al (1972). If the grouped equations (6) are differentiated and integrated, with respect to time, it is possible to obtain expressions for the accelerations of the ultimate velocities as well as the distance traveled by the droplet from the outlet orifice of the nozzle successively over a given period of time.

Given below are only the equations for the droplet's final velocity, V_f and the distance, S traveled from the nozzle outlet orifice as developed by Bernacki et al (1972) for the various flow types.

For laminar or flow in Stokes law region:

$$\left.\begin{aligned} V_f &= V_o \exp\left(\frac{-18\eta_a t}{D_p^2\rho_l}\right) \\ S &= \frac{D_p^2\rho_l}{18\eta_a V_0^2}\left[1 - \exp\left(\frac{-18\eta_a t}{D_p^2\rho_l}\right)\right] \end{aligned}\right\} \quad (7)$$

For transitional or Allen flow region:

$$\left.\begin{aligned} V_f &= \frac{1}{\frac{0.01\rho_a D_p}{\eta_a} + \frac{1}{V_0}\exp\left(\frac{18\eta_a t}{D_p^2\rho_l}\right) - \frac{0.01D_p\rho_a}{\eta_a}} \\ S &= \frac{D_p\rho_l}{0.3\rho_a}\ln\left\{1 + \frac{0.01D_p\rho_a}{\eta_a}V_0\left[1 - \exp\left(\frac{30\eta_a t}{D_p 2\rho_l}\right)\right]\right\} \end{aligned}\right\} \quad (8)$$

For turbulent flow:

$$\left.\begin{aligned} V_f &= \frac{V_0}{1+\frac{0.33\rho_a}{D_p\rho_l}V_o t} \\ S &= \frac{D_p\rho_l}{0.33\rho_a}\ln\left(1+\frac{0.33\rho_a}{D_p\rho_l}V_o t\right) \end{aligned}\right\} \quad (9)$$

By making the simplifying assumption that the entire pressure energy on the liquid content of the nozzle before atomization will be converted into kinetic energy after atomization, Lefebvre (1989) derived the following equation for the initial droplet velocity at the nozzle exit orifice as a function of the nozzle supply pressure and liquid density:

$$V_0 = \sqrt{\frac{2P_l}{\rho_l}} \quad (10)$$

2.2 Model Development

The results of literature search revealed that the fundamental laws underlying the movement of liquid droplets in air are not yet fully understood. To fully understand this phenomenon, equations (1) to (9) which constitute particle dynamics equations and equations of dynamic systems in liquid droplet distribution at high pressure obtained from literature were used to model theoretically the motion phenomenon of liquid droplets in still air.

A computer programme in C++ language, whose flowchart is shown in figure 3, was developed to implement the model to simulate the post-exit behaviour of moving liquid droplets in still air. Thereafter, extreme conditions that sensitively influenced the motion parameters at high and low nozzle supply pressures, droplet diameters and time interval were identified from the simulation results and noted as the basis for future development of a high pressure agro-forestry swirl nozzle prototype.

The variables used in the programmed models were grouped into independent and dependent variables as follows:

(i) Independent variables

(a) Water density (ρ_l), (b)Air density (ρ_a), (c) Air dynamic viscosity (η_a), (d) Nozzle supply pressure (P), (e) Droplet diameter (D_p), (f) Time interval (t).

(ii) Dependent variables

(a) Ultimate velocity (V_u), (b) Final velocity (V_f), (c) Drag force (F_D), (e) Distance (S), (f) Drag coefficient (C_d), Reynolds number (R_e), Droplet exit velocity (V_0).

(iii)Input data

The following input data values obtained from literature were used as recommended by Womac and Bui (2001):

Water density (ρ_ℓ) = 1000 kg/m^3; air density (ρ_a) = 1.225 kg/m^3; air dynamic viscosity (η_a) = 1.789E-05 kPa.sec.

(iv) Assumptions

The following simplifying assumptions were made before developing the model:

(a) Evaporation of the droplets resulting in their drying up during spraying did not occur;
(b) The other external forces known to act on a moving droplet which include Van der Waal's force, thermophoresis, diffusiophoresis, photophoresis, the Basset effect, and forces due to external electrical and pressure gradient were non-existent;
(c) The liquid stream was not set in rotary motion.

These calculations were found to be fairly complicated and troublesome because one could easily run into infinity if care was not taken in selecting the values of t. The problem was averted by starting the simulation at a value of t very close to zero but not zero so that the behaviour of the model in this region could be observed. The time, t was allowed to increase in steps of 0.0198sec starting from 0.01 to 1.188 making a total of six steps. The value of t was not used beyond 1.188sec because t<1.0 sec is the area where it is very difficult to calculate manually. Hence only few steps were taken over and above t = 1.0 sec.

All the four simulated dependent variables were obtained for ten droplet diameters of 100, 200, 300, 400, 500, 600, 700, 800, 900 and 1000 microns. The movement of the droplets was assumed to be in the direction of the positive x-axis with the x-axis in the horizontal direction. The range of droplet diameters selected for the simulation were selected because, with the exception of the 100 micron droplets, they all fell within the range of droplet diameters produced by pressure nozzles without the use of auxiliary air stream as explained by Bernacki et al, (1972); (Klenin et.al,1985). The flowchart for the interactive computer programme is shown in figure 1.

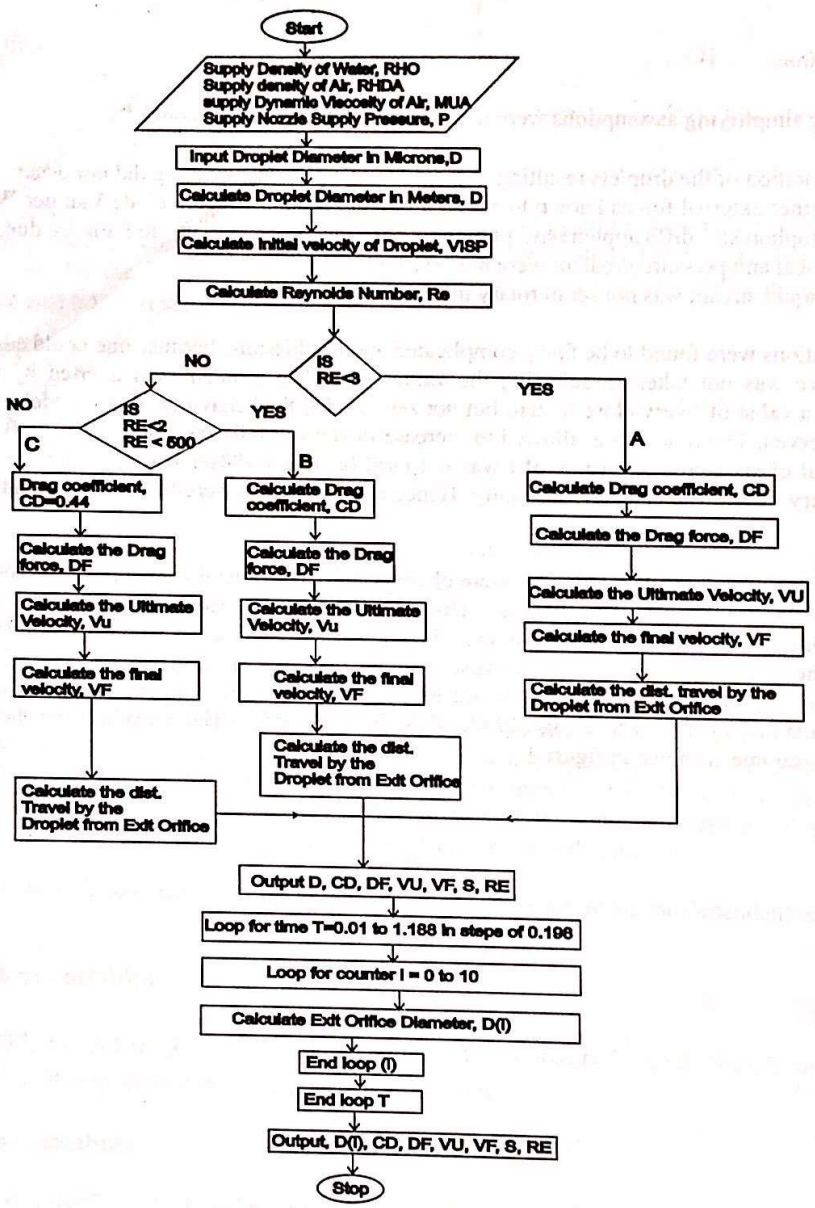

Figure 1. Flowchart for the algorithm to simulate the post exit motion of liquid droplet in still air

3. RESULTS AND DISCUSSION

The simulation results of the movement of the liquid droplets in still air after escaping from the nozzle exit orifice are as shown in the plotted charts in Figures 2 to 7.

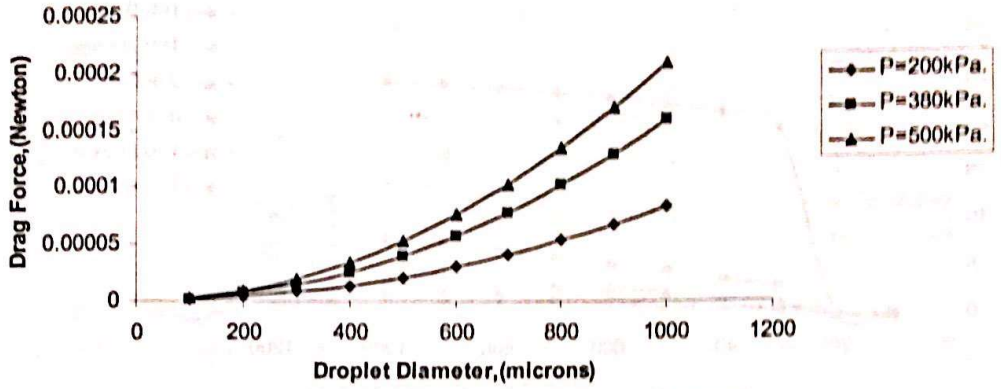

Figure 2 Effect of droplet diameter and nozzle supply pressure on drag force

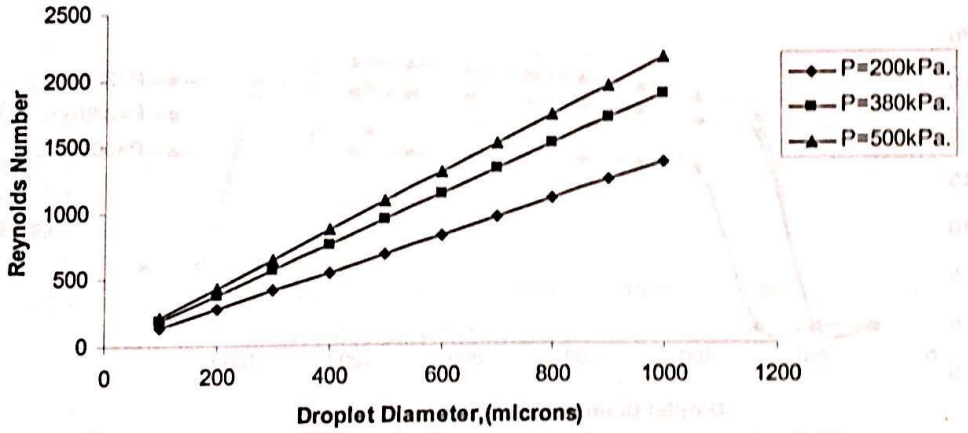

Figure 3: Effect of droplet diameter and nozzle supply pressure on Reynolds number

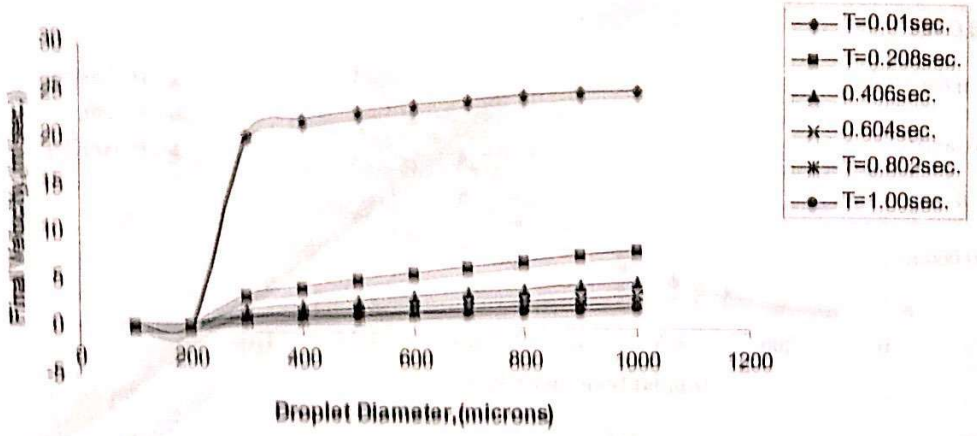

Figure 4: Effect of droplet diameter and time on final velocity

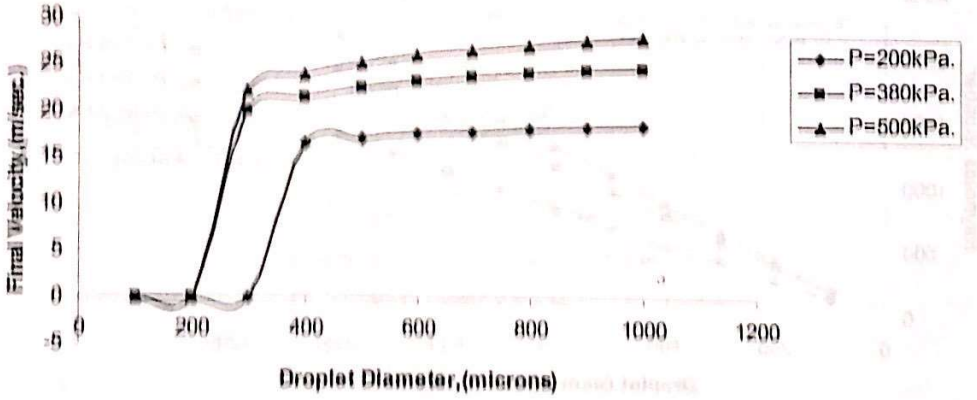

Figure 5: Effect of droplet diameter and nozzle supply pressure on final velocity

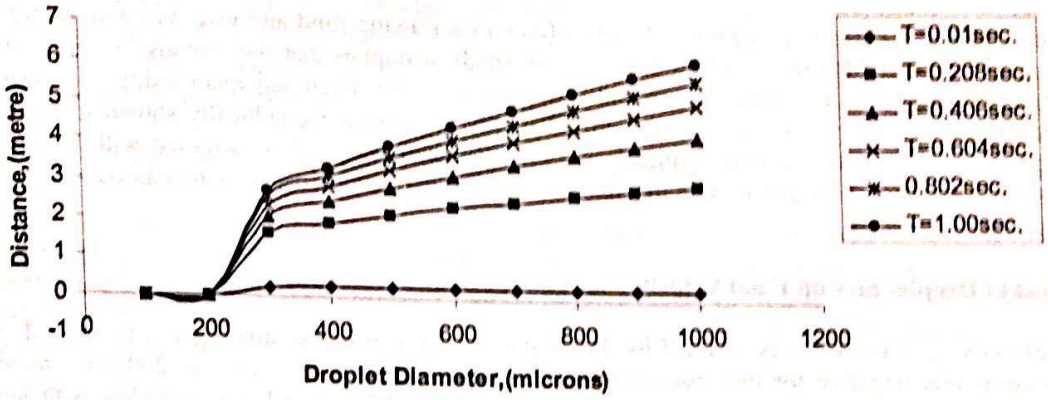

Figure 6: Effect of droplet diameter and time on distance traveled by droplet

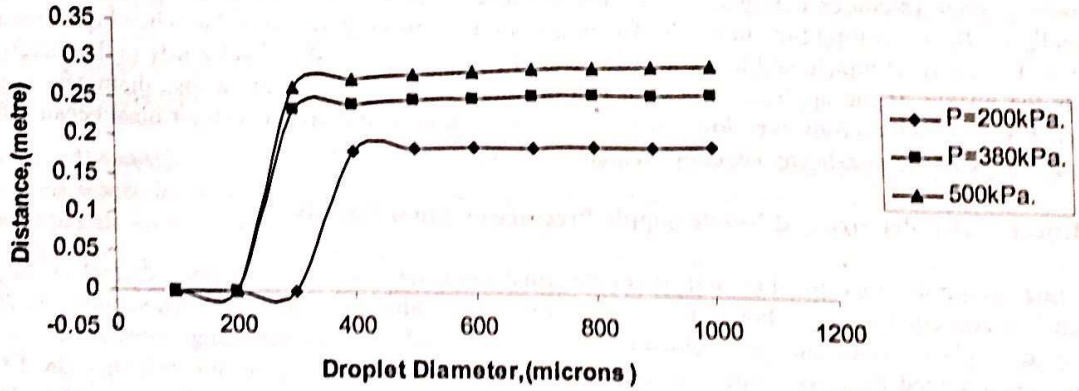

Figure 7: Effect of droplet diameter and nozzle supply pressure on distance traveled by droplets

3.1 Effect of Droplet Size and Nozzle Supply Pressure on Drag Force

The drag force on the droplets increased at an increasing rate as the droplet diameter increased. It also increased as the nozzle supply pressure increased for any level of simulated droplet diameter. For those droplets with droplet diameters between 100 and 200 microns, both the nozzle supply pressure and droplet diameters did not influence the drag force experienced by the moving droplet. This is sequel to the fact that the relationship between the drag force and the droplet diameter is a quadratic function. From the result shown in Figure 2, when the droplet diameter was 100 microns, the drag force on it was only 2.2E-06 Newton; for a droplet diameter of 1000 microns, the drag force increased to 1.61E-4Newton.

3.2 Effect of Droplet Size and Nozzle Supply Pressure on Reynolds Number

Reynolds number is defined as the ratio of inertia force of a flowing fluid and viscous (or skin force) of the fluid. If the Reynolds number of the flow is very small, it implies that the viscous forces are much more predominant than the inertial forces and vice – versa. The functional relationships between the Reynolds number, droplet diameter and the nozzle supply pressure are graphically shown in Figure 3. Although Reynolds number increased linearly with droplet diameter, it also increased with increase in nozzle supply pressure. This implies that the inertial forces on the moving droplets increased as the nozzle supply pressure increased.

3.3 Effect of Droplet Size on Final Velocity

The final velocity is the velocity attained by the droplets at the end of the simulated time interval. The final velocity was negative for the droplets whose diameters fell between 100 and 200 microns after which it started increasing positively at a constant rate (i.e. linearly) for all other droplets with larger diameters. The velocity increased at a constant rate for the droplets whose diameters fell between 200microns and 300microns beyond which it started increasing at a reduced constant rate (i.e. linearly) for all other droplets with larger diameter droplets.

3.3.1 Effect of Droplet Size and Time on Final Velocity

As the time interval increased, the trend of increase in final velocity was maintained although the final velocity values fell sharply for all the simulated sizes of droplets during the second time interval. The reduction in final velocities continued for all the simulated droplet sizes as time progressed, although marginally for the remaining time intervals. The implication of this observation is that when liquid stream discharge from a swirl nozzle and break into droplets, the small droplets flow backwards in the direction towards the nozzle. If the application is such that demands the use of droplets whose diameters range between 100 and 200 microns even lower than the range there is need to assist with air blast because the pressure energy of the nozzle can never be enough.

3.3.2 Effect of Droplet Size and Nozzle Supply Pressure on Final Velocity

The nozzle supply pressure does not affect the final velocities of droplets whose diameters range between 100 and 200microns although they assumed negative values as in the previous section. At 200 kPa nozzle supply pressure, the final velocities of the droplets whose diameters range between 200 and 300 microns assumed negative values. As the droplet diameter increased up to 400 microns, the final velocity increased linearly and increased at a lower rate beyond the 400 micron diameter up to 500 microns beyond which it was increasing at a much lower linear rate up to the maximum simulated droplet diameter of 1000 microns.

The final velocity increased with increase in nozzle supply pressure, although maintaining the same pattern of increase at the lowest simulated nozzle supply pressure (Figure 5).

3.4. Effect of Droplet Size on Distance

The results of the simulation of the programmed model of the distance traveled by the droplets at the end of the simulated time intervals are shown in Figures 6 and 7.

3.4.1 Effect of Droplet Size and Time on Distance

The 100 and 200 micron diameter droplets did not produce any motion when discharged from the nozzle. The droplets whose diameters ranged between these two values moved in the opposite direction (i.e. towards the nozzle) throughout the simulated time intervals. The distance covered by the droplets

increased with time as well as with increase in droplet diameters. The distance covered by the droplets over a time interval of 0.01second was about the same for all the droplets with 300 micron diameter and above. The distance covered by the droplets whose diameter ranged between 200 and 300 microns was very marginal regardless of the interval of time which elapsed. This is probably due to the earlier established fact that inertial forces have very little or no effect on the small diameter droplets because it was the viscous forces that were predominant during their motions(figure 6).

3.4.2 Effect of Droplet Size and Nozzle Supply Pressure on Distance

The results shown in Figure 7 reveal that the pattern of variation of distance with droplet diameter and nozzle supply pressure is exactly as obtained for final velocity. This simply corroborates the fact that once there is no velocity there can be no displacement (or covered distance). Nozzle discharge with high nozzle supply pressure will result in higher covered distance by the droplets. In other words, higher pressure means higher penetration range for the droplets.

These observations are consistent with those reported by Womac and Bui (2001) as well as Sidahmed, (1996). The larger droplets like their smaller counterparts also lose momentum during their movement in still air; however, they did not spread over a wide area as those with small diameters. Hence, in order to obtain a wider swath from a swirl nozzle, liquid droplets composed of small diameter droplets should be preferred.

4. CONCLUSIONS

The drag force increased with increase in droplet diameter and nozzle supply pressure. For a ten-fold increase in droplet diameter, drag force increases by seventy three times over and above that of the initial droplet diameter. When small diameter droplets move in still air, viscous forces are predominant on them. As the droplet diameters increase, the viscous forces become exchanged for the inertial forces until they become predominant when the droplet diameters become large.

The predominance of viscous forces on droplets with small diameter assumed extreme limit on those droplets whose diameters were 200 microns or less; these droplets developed negative displacements and velocities as soon as they were discharged from the nozzle exit orifice. In other words, instead of the droplets moving away from the nozzle exit orifice after escaping from the nozzle, they will move backwards towards the nozzle. This phenomenon will occur regardless of the nozzle supply pressure. As the droplet diameter increased in size from 200 microns, the final velocities of the moving droplets starts increasing in magnitude until 400 micron droplet diameters when the rate of increase became nearly zero. At this level, final velocities became nearly constant as the droplet diameter increased. For any particular droplet diameter within this size range any increase in nozzle supply pressure increases the final velocity. the pattern of variation of distance covered by the droplets is very similar to that of final velocity variation in terms of nozzle supply pressure and droplet diameter. The final velocity fell sharply from the maximum value 30 m/sec for a 1000 micron diameter droplet when the nozzle supply pressure was 500kPa to 16 m/sec when the nozzle supply pressure was reduced to 200kPa. Similarly for the 1000micron diameter droplet, the distance covered during the time interval of 0.1sec when the nozzle supply pressure was 500kPa fell from 0.31 m to 0.17 m when the nozzle supply pressure was reduced to 200kPa.

REFERENCES

Adejumo, T. O. 2005. Crop protection strategies for major diseases of cocoa, coffee and cashew in Nigeria. African Journal of Biotechnology, 4(2):143-150.

ASAE S572. 2002. Spray nozzle classification by droplet spectra. ASAE S572 Aug., 99, ASAE Standards 2002-49th Edition, Standards, Engineering Practices Data. ASAE. St. Joseph, Michigan.

Awardy, M. N. El – 1978. An atomization theory for swirl nozzles. Transactions of the ASAE. 21(1): 70 – 74.

Balagurusamy, E. 2004. Object-oriented programming with C++. Second Edition. Tata McGraw-Hill Publishing Company Ltd.

Bernacki, H., Haman, J. and Kanafojski, C.Z. 1972. Agricultural Machines. 1:780-812. National Technical Information Service. U. S. Department of Commerce. VA 22161.

Bode, L. E., Langley, T. E., and Butler, B. J. 1979. Performance characteristics of y-pass spray nozzles. Transactions of the ASAE 22:1016-1022.

Bowers, J. H., Bailey, B. A., Hebbar, P. K., Sanogo, S., Lumsden, R. D. 2001. The impact of plant diseases on world chocolate production online. Plant Health Progress doc: 10.1094/PHP – 2001 – 0709 – 01 – RK.

Goering, C. E., Ode, L. E. and Gebhardt, M. R. 1972. Mathematical modeling of spray droplet deceleration and evaporation. Transactions of the ASAE 15(10): 220 – 225.

Kang, B.T. 1996. Sustainable agroforestry systems for the tropics: concepts and examples. IITA Research Guide 26.IITA Training Program. IITA, Ibadan.

Klenin, N. I., Popov, I. F., and Sakun, V. A. 1985. Agricultural Machines. Amerind Publishing Co. Pvt. Ltd. New Delhi.

Koo, Y. M. and Kuhlman. 1993. Theoretical spray performance of swirl-type nozzles. Transactions of the ASAE. 36(3):671–678.

Lefebvre, A. H. 1989. Atomization and Sprays. (Combustion: An International Series). Taylor and Francis Publishers, New York.

Osarenren J. O., and Ndukwe, G. U. 2002. Nozzle spray performance analyser. Paper No. 021028 ASAE. St. Joseph. Mich. 49085. U.S.A.

Rajankumar. 2007. Agroforestry. Wikipedia Free Encyclopedia.

Shaip, B., Aliyu, A., Bakshi, J.S. 1997. Nigerian National Agricultural Research Strategy Plan 1996-2010. Department of Agricultural Sciences, Federal Ministry of Agriculture and Natural Resources

Sidahmed, M. M. 1996. A Theory for Predicting the size and velocity of droplets from pressure nozzles. Transactions of the ASAE. 39(2):385–391.

Taiwo, A. 2009. A study of some operating parameters of a high pressure agro-forestry swirl nozzle. An Unpublished Ph.D. Thesis Submitted to the Department of Agricultural and Biosystems Engineering, University of Ilorin, Ilorin, Kwara State, Nigeria.

United Nation Environmental Programme 2008. The Billion tree Campaign. ICRAF Director General's Statement.

United Nations Conference on Trade and Environment. 2006. Trade and Environment Review. UNCTAD.

Womac, A. R. and Bui, Q. D. 2001. Development of a variable flow rate fan spray nozzle for precision chemical application. Paper No. 011078. ASABE. St. Joseph. MI.

Zhu, H., Reichard, D.L., Fox, R. D., Brazee, R. D. and Ozkan, H. E. 1994. Simulation of Drift of Discreet Sizes of Water Droplets from field sprayers. Transactions of the ASAE. 37(5): 1401 – 407.